

Extraordinary centromeres: differences in the meiotic chromosomes of two rock lizards species *Darevskia portschinskii* and *Darevskia raddei*

Victor Spangenberg ^{Corresp., 1}, Marine Arakelyan ², Eduard Galoyan ³, Mark Pankin ¹, Ruzanna Petrosyan ², Ilona Stepanyan ⁴, Tatiana Grishaeva ¹, Felix Danielyan ², Oxana Kolomiets ¹

¹ Vavilov Institute of General Genetics, Moscow, Russian Federation

² Department of Zoology, Yerevan State University, Yerevan, Armenia

³ Zoological Museum, Moscow State University, Moscow, Russia

⁴ Scientific Center of Zoology and Hydroecology, Yerevan, Armenia

Corresponding Author: Victor Spangenberg

Email address: spangenberg@vigg.ru

According to the synthesis of 30 years of multidisciplinary studies parthenogenetic species of rock lizards of genus *Darevskia* were formed as a result of different combination patterns of interspecific hybridization of the four bisexual parental species: *D. raddei*, *D. mixta*, *D. valentini*, and *D. portschinskii*. In particular *D. portschinskii* and *D. raddei* are considered as the parental species for the parthenogenetic species *D. rostombekowi*. Here for the first time we present the result of comparative immunocytochemical study of primary spermatocyte nuclei spreads from the leptotene to diplotene stages of meiotic prophase I in two species: *D. portschinskii* and *D. raddei*. We observed similar chromosome lengths for both synaptonemal complex (SC) karyotypes as well as similar number of crossing over sites. However, unexpected differences in the number and distribution of anti-centromere antibody (ACA) foci were detected in the SC structure of bivalents of the two species. In all examined *D. portschinskii* spermatocyte nuclei, one immunostained centromere focus was detected per SC bivalent. In contrast, in almost every studied *D. raddei* nuclei we identified three - nine SCs with additional immunostained ACA foci per SC bivalent. Thus, the obtained results allow us to identify species-specific karyotype features, previously not been detected using conventional mitotic chromosome analysis. Presumably the additional centromere foci are result of epigenetic chromatin modifications. We assume that this characteristic of the *D. raddei* karyotype could represent useful marker for the future studies of parthenogenetic species hybrid karyotypes related to *D. raddei*.

1 **Extraordinary centromeres: differences in the meiotic**
2 **chromosomes of two rock lizards species *Darevskia***
3 ***portschinskii* and *Darevskia raddei***

4

5 Victor Spangenberg^{1*}, Marine Arakelyan², Eduard Galoyan³, Mark Pankin¹, Ruzanna Petrosyan²,
6 Ilona Stepanyan⁴, Tatiana Grishaeva¹, Felix Danielyan² and Oxana Kolomiets¹

7

8 ¹ Vavilov Institute of General Genetics, Russian Academy of Sciences, Moscow 119991,

9 ² Department of Zoology, Yerevan State University, Yerevan 0025, Armenia

10 ³ Zoological Museum, Lomonosov Moscow State University, Moscow 125009, Russia

11 ⁴ Scientific Center of Zoology and Hydroecology NAS RA, 0014, Yerevan, Armenia

12

13 Corresponding Author:

14 Victor Spangenberg

15 Gubkin 3, Moscow, 119991, Russia

16 Email address: v.spangenberg@gmail.com

17

18 **Abstract**

19 According to the synthesis of 30 years of multidisciplinary studies parthenogenetic species of
20 rock lizards of genus *Darevskia* were formed as a result of different combination patterns of
21 interspecific hybridization of the four bisexual parental species: *D. raddei*, *D. mixta*, *D.*
22 *valentini*, and *D. portschinskii*. In particular *D. portschinskii* and *D. raddei* are considered as
23 the parental species for the parthenogenetic species *D. rostombekowi*. Here for the first time we
24 present the result of comparative immunocytochemical study of primary spermatocyte nuclei
25 spreads from the leptotene to diplotene stages of meiotic prophase I in two species: *D.*
26 *portschinskii* and *D. raddei*. We observed similar chromosome lengths for both synaptonemal
27 complex (SC) karyotypes as well as similar number of crossing over sites. However,
28 unexpected differences in the number and distribution of anti-centromere antibody (ACA) foci
29 were detected in the SC structure of bivalents of the two species. In all examined *D.*
30 *portschinskii* spermatocyte nuclei, one immunostained centromere focus was detected per SC
31 bivalent. In contrast, in almost every studied *D. raddei* nuclei we identified three – nine SCs
32 with additional immunostained ACA foci per SC bivalent. Thus, the obtained results allow us to
33 identify species-specific karyotype features, previously not been detected using conventional
34 mitotic chromosome analysis. Presumably the additional centromere foci are result of
35 epigenetic chromatin modifications. We assume that this characteristic of the *D. raddei*
36 karyotype could represent useful marker for the future studies of parthenogenetic species hybrid
37 karyotypes related to *D. raddei*.

38

39 **Introduction**

40 According to the results of long term fundamental international studies initiated by I.S.
41 Darevsky [1,2,3,4] convincing evidence has been obtained that seven diploid parthenogenetic
42 species of lizards of the *Darevskia* genus have resulted from hybridogenous speciation

43 [5,6,7,8,9,10,11,12]. The origin of parthenogenetic species from the hybridization of bisexual
44 species has been confirmed from detailed studies of skin transplantation [13,14,15], allozyme
45 data [7,9,16,17,18], mitochondrial [6,8,10,19] and nuclear DNA sequences [11,12,20,21,22,23].

46 The balance hypothesis suggest that there is a narrow range of genetic divergence between
47 parental species within which F1 hybrids have a probability of establishing parthenogenetic form
48 [9,24].

49 In this study, we performed a detailed analysis of the meiotic prophase I stages in of two
50 species: *D. portschinskii* and *D. raddei* which are parental for the parthenogenetic species *D.*
51 *rostombekowi*. Previous cytogenetic studies of these two species were made using light
52 microscopy on mitotic and meiotic metaphase plates [25,26] and are sporadic. Here we represent
53 detailed comparative cytogenetic study of synaptonemal complexes karyotypes (SC karyotypes)
54 using spread preparation and immuno-FISH technique. This approach provides visualization of
55 meiotic SC bivalents which are 3-5 times longer than mitotic metaphase chromosomes and
56 makes it possible to discover chromosomal rearrangements that are undetectable at diakinesis
57 and metaphase I [27]. Additional information can also be obtained: precise localization of
58 centromeres, distribution of crossing over sites and telomere DNA-repeats in the structure of
59 meiotic chromosomes.

60

61 **Materials & Methods**

62 Four adult animals were captured and examined in May 2017 and two in September 2017
63 and were deposited in the research collection of the Zoological Museum of Lomonosov Moscow
64 State University (ZMMU). One male *D. raddei* (Zuar population, ZMMU R-15598, specimen
65 VS0029) collected by E.A. Galoyan and V.E. Spangenberg in May 2017, one male *D. raddei*
66 (Zuar population, ZMMU R-15599, specimen VS0039) collected by M.S. Arakelyan and V.E.
67 Spangenberg in September 2017) and two males *D. portchinskii* (Zuar population, ZMMU R-
68 15600, specimen VS0028, ZMMU R-15600, specimen VS0050) collected by M.S. Arakelyan,
69 E.A. Galoyan and V. E. Spangenberg in May and September 2017 respectively. The
70 manipulations of the animals followed international rules of the Manual on Humane Use of
71 Animals in Biomedical Research and the rules of the Ethics Committee for Animal Research of
72 the Vavilov Institute of General Genetics (protocol No. 3 from November 10 2016).

73 Spread synaptonemal complex (SC) preparations were prepared and fixed using the
74 technique of Navarro et al. [28]. Poly-L-lysine-coated slides were used for all
75 immunofluorescence studies. The slides were washed with phosphate-buffered saline (PBS) and
76 incubated overnight at 4°C with primary antibodies diluted in antibody dilution buffer (ADB: 3%
77 bovine serum albumin (BSA), 0.05% Triton X-100 in PBS).

78 SCs were detected by rabbit polyclonal antibodies to the SC and axial element protein
79 SYCP3 (1:250, Abcam, UK), centromeres were detected by anti-kinetochore proteins antibodies
80 ACA (1:500, Antibodies Incorporated, USA). The late recombination nodules (sites of crossing
81 over) were detected using mouse monoclonal antibodies to the DNA mismatch repair protein -
82 MLH1 (1:250, Abcam, UK). After washing, we used the secondary antibodies diluted in ADB:
83 goat anti mouse Immunoglobulin IgG, Alexa Fluor 555 (1:500, Abcam, UK), Rhodamine-
84 conjugated chicken anti-rabbit IgG (1:400, Santa Cruz Biotechnology, USA), FITC-conjugated
85 goat anti-rabbit IgG (1:500, Jackson ImmunoResearch, USA), goat anti-rabbit Alexa Fluor 488
86 (1:500, Invitrogen, USA), goat anti-human Alexa Fluor 546 (1:500, Invitrogen, USA).
87 Secondary antibody incubations were performed in a humid chamber at 37°C for 2h. Mitotic
88 chromosomes were prepared from bone marrow and spleen following Ford and Hamerton with

89 modifications and fixed in an ice-cold acetic acid–methanol solution (1:3) [29]. Telomere FISH
90 probe (Telomere PNA FISH Kit/FITC, Dako, K5325) was used according to the manufacturer
91 protocol.

92 The slides were examined using an AxioImager D1 microscope (Carl Zeiss, Germany)
93 equipped with an Axiocam HRm CCD camera (Carl Zeiss, Germany), Carl Zeiss filter sets
94 (FS01, FS38HE, and FS43HE) and image-processing AxioVision Release 4.6.3. software (Carl
95 Zeiss, Germany). All preparations were mounted in Vectashield antifade mounting medium with
96 DAPI (Vector Laboratories, USA). CENP proteins were compared by alignment (COBALT
97 software program, <http://www.ncbi.nlm.nih.gov/tools/cobalt/cobalt.cgi?CMD=Web>).

98 Prophase I stages were determined by the analysis of the combination of basic
99 morphological criteria used in studies of meiotic cells [30,31]. The rock lizards-specific features
100 of the prophase I stages were described before (Spangenberg et. al 2017). Early presynaptic
101 stages criteria for leptotene: multiple fragments of unpaired axial elements, and for the
102 zygotene: long partially synapsed axial elements, «bouquet» formation (telomere clustering at
103 zygotene), no signes of desynapsis in telomere regions, no MLH1-protein foci. Mid-prophase I
104 stage (pachytene) criteria: complete homologous chromosome synapsis, non-fragmented lateral
105 elements of synaptonemal complexes, shortened SCs, MLH1-protein foci. Postsynaptic stage
106 (diplotene) criteria: signs of synaptonemal complexes disassembly (lateral elements desynapsis
107 start in peritelomeric or interstitial regions, elongation and fragmentation), MLH1-protein foci
108 maintenance.

109

110 Results

111 *Early stages of meiotic prophase I in D. portschinskii and D. raddei: leptotene and zygotene.*

112

113 In both species *D. portschinskii* and *D. raddei*, leptotene begins with the formation of axial
114 structures, which resemble dotted lines (Fig. 1 A, B) until the early zygotene (Fig. 1 C, D).
115 Assembly of chromosome axial structures from the fragments was often observed together with
116 the beginning of homologous synapsis (early “bouquet” formation) in different zones of one
117 nucleus (Fig. 1 C, D). Immunostaining of kinetochore proteins revealed progressive clustering of
118 the centromeres of all 38 acrocentric chromosomes from the leptotene to early zygotene stages in
119 both species (Fig. 1 C, D).

120

121 Our detailed study of early prophase I stages (preceding the pachytene) revealed previously
122 unknown phenomenon specific for *D. raddei* – additional foci of anti-kinetochore
123 proteins antibodies ACA (Fig. 1 B, D). Additional ACA foci were detected on the still
124 unsynapsed axial elements of *D. raddei* homologous chromosomes at zygotene stage (Fig. 2 A,
125 D). Thus four ACA foci were visible on several SC bivalents during the synapsis, with two on
126 each axial element (Fig. 2 B, C, E). Totally in 26 of 30 leptotene-zygotene nuclei studied 1 – 4
127 additional centromere signals were detected in both *D. raddei* individuals. Fragmented axial
128 cores of chromosomes at the presynaptic stages (before the pachytene) did not allow us to study
129 actual number and distribution of additional ACA foci among the meiotic chromosomes. The
130 next meiotic prophase I stage, pachytene, was analysed in details due to complete synaptonemal
131 complexes assembly and applicability for the distinct chromosomes identification.

132

133 *Late stages of meiotic prophase I in D. portschinskii and D. raddei: pachytene and diplotene.*

134

135 The pachytene stage of both species studied (*D. portschinskii* and *D. raddei*) is characterised
136 by complete synapsis of all 19 acrocentric SC bivalents (18 autosomal bivalents and the ZZ sex
137 bivalent) (Fig. 3 A, B).

138

139 In *D. portschinskii* pachytene nuclei single ACA focus was detected at one end of each of
140 the 19 SCs (78 nuclei studied) (Fig. 3 A). However in *D. raddei* apart from to the usual 19 ACA
141 foci on the SC ends we detected additional ACA foci on the SC bivalents (Fig. 3 B). These
142 signals were located closely in the SC structure at a distance of 0.27–1.39 μm , on average
143 0.62 ± 0.21 (mean \pm SD, 54 nuclei studied) and demonstrated similar or slightly different signal
144 intensities.

145 Pachytene stage was the most representative for the precise chromosome length
146 measurements, other prophase I stages are inapplicable to this study. Nevertheless synaptonemal
147 complex karyotyping revealed minor differences in the length of medium-sized SC bivalents in
148 both species (Fig. 4 A) making the identification of distinct dicentric (Fig. 4 C) chromosomes
149 more challenging.

150 We performed the detailed analysis of 54 pachytene nuclei of the six preparations from two
151 *D. raddei* animals. We selected immunostained SC-karyotypes without bivalent overlapping and
152 used relative chromosomes length in order to minimize possible influence of the different
153 spreading conditions between nuclei studied. Additional ACA foci were detected at
154 chromosomes 1-17 with enrichment on chromosomes 1 – 4 (1 – 90.7%; 2 – 79.6%; 3 – 88.9%;
155 4 – 63.0% of all 54 nuclei studied), medium occurrence on chromosomes 5 – 14 (5 – 29.6%; 6 –
156 24.1%; 7 – 29.6%; 8 – 16.7%; 9 – 20.4%; 10 – 11.1%; 11 – 20.4%; 12 – 25.9%; 13 – 24.1%; 14
157 – 29.6% of 54 nuclei studied), sporadic occurrence on chromosomes 15 – 17 (15 – 3.7%; 16 –
158 1.9%; 17 – 5.6% of 54 nuclei studied) and not been detected on the chromosomes 18 and 19
159 (Fig. 4 D, E).

160 In total, additional ACA foci were detected in 198 out of the 211 *D. raddei* primary
161 spermatocyte nuclei studied (leptotene-diplotene stages).

162

163 ***FISH with telomere DNA-probes on pachytene chromosomes of D. portschinskii and D.*** 164 ***raddei.***

165 Fluorescent *in situ* hybridization (FISH) with telomere probes (Fig. 4 B, C) revealed a
166 standard distribution of telomere repeats in the SC karyotypes of *D. portschinskii* and *D. raddei*,
167 with no interstitial signals [32] detected in the pachytene SC bivalents (25 nuclei for each species
168 studied). In particular, we studied the SC regions of additional ACA foci in *D. raddei* SC
169 bivalents, and no one telomere FISH-signal was detected at any of these locations in all nuclei
170 studied (Fig. 4C).

171

172 ***Immunodetection of crossing over sites in D. portschinskii and D. raddei spermatocytes I*** 173

173

174 Immunolocalization of the MLH1 protein (late recombination nodules marker, prospective
175 chiasmata) on pachytene stage in the SC preparations was performed for both species (Fig. 5 A,
176 B). The average number of crossing over sites (MLH1 foci) was 28.43 ± 2.11 (mean \pm SD) in *D.*
177 *portschinskii* (Fig. 5 C) and 28.64 ± 2.07 (mean \pm SD) in *D. raddei* (Fig. 5 C). We did not detect
178 MLH1 foci in the SC regions between the two ACA foci in all 55 immunostained *D. raddei*
179 spermatocyte I nuclei (Fig. 5 B).

180

181 **Discussion**

182

183 ***Synaptonemal complex processing and number of crossing over sites during prophase I for *D.****
184 ***portschinskii* and *D. raddei***

185 In general, the characteristics of the stages of meiotic prophase I were similar between
186 species (Fig. 1; Fig. 3), and were comparable to the results of our previous study of two other
187 bisexual species, *D. raddei nairensis* and *D. valentini* [33]. For example, the absence of a
188 classical leptotene stage with long threads (presynaptic stage with completely formed
189 chromosome axial elements) is a common feature among all four rock lizards species studied by
190 us to date. Furthermore, early zygotene, organization of “bouquet” formation, progression of
191 axial element synapsis during zygotene and SC assembly at pachytene were similar in both
192 species (Fig. 1 C, D and Fig. 3 A, B). No significant difference in numbers of crossing over sites
193 was detected between *D. portschinskii* and *D. raddei* males (Fig. 5 C) in the studied population.

194

195 ***Extraordinary difference of distribution of ACA foci in the SC bivalents in *D. portschinskii****
196 ***and *D. raddei****

197

198 As visible in our results, the SC karyotypes of the two species display a striking difference
199 in relation to the immunostaining of kinetochore proteins. Two ACA foci can be observed in the
200 structure of SC bivalents 1-17 in primary spermatocyte nuclei of *D. raddei* (Fig. 4 D, E), one
201 near the telomere, similar to the acrocentric organization of SCs in *D. portschinskii*, and the
202 second located at some distance along the SC axis (Fig. 4 C). Spreading technique allow us to
203 study meiotic chromosomes in detail (Fig. 4 C) and to detect additional ACA foci. This
204 phenomenon has not been previously described in mitotic chromosomes due to high levels of
205 chromatin compaction as well as in previous studies of the meiotic chromosome structure of rock
206 lizards using light microscopy [25,26].

207 Immunodetection of additional ACA foci in *D. raddei* during the leptotene and zygotene
208 stages indicates the presence of two ACA foci in both homologous chromosomes prior to
209 synapsis (Fig. 1 B, D; Fig. 2 B, C, E).

210 The differences in additional ACA foci number and distribution were detected in the nuclei
211 from one sample preparation as well as between preparation slides derived from different *D.*
212 *raddei* animals. We suppose that this result can be explained by the fact that closely located
213 double ACA foci often can sometimes not been distinguished from enlarged (or elliptical) single
214 focus due to limitations of fluorescence microscopy as well as nearest chromosome lengths are
215 very close in this species (Fig. 4 A). On the other hand the different chromosome numbers with
216 additional ACA foci from the one sample could indicate on the high level of instability of
217 centromere proteins distribution in the pericentromeric regions in *D. raddei*.

218 Additional ACA foci we have detected in SC-karyotype of *D. raddei* males leads us to
219 assume that the formation of the additional foci occurred not via inversions or duplication but via
220 an epigenetic mechanism in these species. This is supported by the fact that we did not observed
221 any disruption of synapsis or inversion loops in the pericentromeric regions of SC bivalents with
222 additional ACA foci in all 198 nuclei studied.

223 In recent years, studies in mammals have reported that neocentromeres can be formed in
224 intact chromosomes (without rearrangements), which can functionally replace the native
225 centromere [34]. *De novo* centromere formation occurs by an epigenetic sequence-independent

226 mechanism involving the deposition of a centromere-specific histone H3 variant, CENP-A
227 [35,36,37]. A study of artificial neocentromere formation in chickens demonstrated that while
228 they can be formed in any region of the chromosome, the most likely location of neocentromere
229 formation is close to the native centromere. The authors suggested that this is due to the potential
230 enrichment of epigenetic marks in the zone of the native centromere [38,39]. According to
231 studies of mitosis in different species, the formation of dicentric chromosomes (chromosomes
232 with two active centromeres) may lead to breakage or loss of such chromosomes during the
233 process of cell division and, consequently, cell death [40,41]. However, dicentric chromosomes
234 can be inherited if one of the centromeres is inactivated without altering the DNA sequence
235 [42,43]. Furthermore, immunocytochemical markers allow the identification of which of the two
236 centromeres is active [44,45]. However, the molecular basis for centromere inactivation is not
237 well understood [40].

238 Our results do not allow the status of additional ACA foci to be determined, specifically
239 whether they are associated with active or inactivated centromeres. However, the number of
240 nuclei with clear additional ACA foci, identified in two *D. raddei* males, indicates that this
241 phenomenon is not random. Moreover, numerous mature elongated spermatids with normal
242 morphology were found in preparations from both *D. raddei* males in the current study. The
243 successful formation of mature germ cells by *D. raddei* males indicates that the peculiarities of
244 centromere organization described above does not affect their fertility.

245 The formation of double centromeres in the structure of SCs has been previously reported
246 for *Danio rerio* fish [46]. In this study, 3–4 double centromeres were detected in the nuclei of
247 primary spermatocytes, which the author characterised as being misaligned centromeres. The
248 author also pointed out that such double centromeres are not necessarily found on the same
249 chromosomes, judging by the length and centromere position [46]. This pattern correlates well
250 with the distribution of the double ACA foci observed for *D. raddei* in the current study.
251 However, in the early zygotene nuclei of *D. raddei* males, we were able to detect two ACA foci
252 on the yet unpaired axial elements of chromosomes. Furthermore, four ACA foci were visible by
253 the zygotene stage, with two on each axial element (Fig. 2 B, C, E). This indicates the presence
254 of two ACA antibody binding sites on each axial element but not incomplete alignment of
255 homologous chromosomes.

256 It should be noted that we used similar antibodies (ACA) to those used by other studies
257 (ACA, CREST) [47,48,49]. The applicability of these antibodies for the detection of centromeres
258 in a wide range of vertebrate species has long been established. In addition, numerous studies in
259 the literature have discussed the specific characteristics of immunostaining using these
260 antibodies during different phases of the cell life cycle [47,49]. Our comparative studies of
261 CENP-A and CENP-C proteins by alignment of amino acids sequences confirmed our negative
262 immunostaining experiments with the commercially available CENP-antibodies. Poor similarity
263 was detected between reptilian proteins and the human immunogen polypeptides used in
264 commercial antibodies.

265 Further studies using monoclonal antibodies against specific proteins are needed in order to
266 distinguish active and inactivated centromeres, in addition to FISH with pericentromeric satellite
267 DNA. An interesting finding was the detection of additional ACA foci in SC preparations of the
268 most closely related species, *D. raddei nairensis* (in supplementary data). *D. raddei* and *D.*
269 *raddei nairensis* are considered recently divergent species, and are actively investigated as a
270 model system for the study of speciation mechanisms [23].

271

272

273 Conclusions

274 Our comparative immunomorphological study revealed that karyotypes of both species were
275 found to be very similar with regard to chromosome length, with similar features related to
276 passage through the stages of meiotic prophase I and the number of crossing over sites.

277 Nevertheless we were able to detect striking difference in the number and distribution of
278 centromere proteins foci of these species: the formation of additional ACA foci in the structure
279 of several SC bivalents in the spermatocyte nuclei of *D. raddei* but not in *D. portschinskii*. It is
280 important to note that additional ACA foci were detected during all stages of meiotic prophase I,
281 including the presynaptic stages, on the yet unpaired axial elements of homologous
282 chromosomes. Thus, we observed SC during the assembly with four ACA foci at the zygotene
283 stage, two on each axial element. This indicates the presence of two ACA antibodies binding
284 sites in the structure of each homologous chromosomes, thus eliminating the idea of incomplete
285 alignment of homologous chromosomes during synapsis or desynapsis.

286 The additional ACA foci observed in the SC structure appeared to result from epigenetic
287 transformations in the chromatin structure of *D. raddei* males, and is not related to chromosomal
288 aberrations. In any case, we did not observed the formation of inversion loops in SC fragments
289 between two ACA foci in any of the 198 studied nuclei (leptotene-diplotene).

290 Further research is needed to determine the possible interpretation of the extraordinary
291 chromosome organization observed in *D. raddei* in relation to the active and surprisingly
292 efficient interspecific hybridization in rock lizards. In particular, a detailed study of the
293 epigenetic chromatin modifications of hybrid animals is required. We assume that this
294 characteristic of the *D. raddei* karyotype could represent useful markers for our future study of
295 diploid parthenogenetic species *D. rostombekowi* karyotype as well as for other unisexual
296 species related to *D. raddei*.

297

298 Acknowledgements

299 We are grateful for the collaboration with prof. Yu. F. Bogdanov, our colleagues A.N.
300 Bogomazova, S.A. Simanovsky, I.S. Mazheika, M.A. Lelekova and A.A. Kashintsova. We thank
301 the Genetic Polymorphisms Core Facility of the Vavilov Institute of General Genetics of the
302 Russian Academy of Sciences, Moscow for the possibility to use their microscopes.

303

304 References

- 305 1. Darevsky, I.S. Natural parthenogenesis in certain subspecies of rock lizards (*Lacerta*
306 *Saxicola* Eversmann). *Doklady Akademii Nauk SSSR* 1958, 122, 730–732. (In Russian)
- 307 2. Darevsky, I.S. Natural parthenogenesis in a polymorphic group of Caucasian rock lizard s
308 related to *Lacerta saxicola* Eversmann. *J. Ohio Herpetol. Soc.* 1966, 5, 114–152.
- 309 3. Darevsky, I.S. Rock lizards of the Caucasus (Systematics, Ecology and Phylogenesi of the
310 polymorphic groups of Rock lizards of the Subgenus *Archaeolacerta*). Nauka press, 1967,
311 Leningrad, 216 pp. [Translation: New Delhi: Indian National Scientific Documentation
312 Centre, 276 pp]
- 313 4. Darevsky, I.S. Evolution and ecology of parthenogenesis in reptiles. *Soc. Study Amphib.*
314 *Reptiles Contr. Herpetol.* 1992, 9, 21–39.
- 315 5. Borkin, L.J.; Darevsky, I.S. Reticular (hybridogeneous) speciation in vertebrate. *Zhurnal*
316 *Obshechi Biol.* 1980, 41, 485–506. (In Russian)

- 317 6. Moritz, C.; Uzzell, T.; Spolsky, C.; Hotz, H.; Darevsky, I.; Kupriyanova, L.; Danielyan, F.
318 The material ancestry and approximate age of parthenogenetic species of Caucasian rock
319 lizards (*Lacerta: Lacertidae*). *Genetica*, 1992, 87, 53–62.
- 320 7. Murphy, R.W.; Darevsky, I.S.; MacCulloch, R.D.; Fu, J.; Kupriyanova, L.A. Evolution of
321 the bisexual species of Caucasian rock lizards: A phylogenetic evaluation of allozyme data.
322 *Russian Journal of Herpetology*, Moscow, 1996, 3 (1): 18-31.
- 323 8. Fu, J. Toward the Phylogeny of the Family *Lacertidae*: Implications from Mitochondrial
324 DNA 12S and 16S Gene Sequences (*Reptilia: Squamata*). *Molecular Phylogenetics and*
325 *Evolution*, 1998, 9 (1): 118-130.
- 326 9. Murphy, R.W.; Fu, J.; MacCulloch, R.D.; Darevsky, I.S.; Kupriyanova, L.A. A fine line
327 between sex and unisexuality: the phylogenetic constrains on parthenogenesis in lacertid
328 lizards. *Zoological Journal of the Linnean Society*, 2000, 130 (4): 527-549.
- 329 10. Fu, J., Murphy, R. W.; Darevsky, I. S. Divergence of the cytochrome b gene in the *Lacerta*
330 *raddei* complex and its parthenogenetic daughter species: evidence for recent multiple
331 origins. *Copeia*, 2000, 2000(2), 432-440.
- 332 11. Freitas, S.; Rocha, S.; Campos, J.; Ahmadzadeh, F.; Corti, C.; Sillero, N.; Ilgaz, C.;
333 Kumlutaş, Y.; Arakelyan, M.; Harris, D.J.; Carretero, M.A. Parthenogenesis through the ice
334 ages: A biogeographic analysis of Caucasian rock lizards (genus *Darevskia*). *Molecular*
335 *Phylogenetics and Evolution*, 2016, 102: 117–127.
- 336 12. Ryskov, A.P.; Osipov, F.A.; Omelchenko, A.V.; Semyenova, S.K.; Girnyk, A.E.; Kochagin,
337 V.I.; Vergun, A.A.; Murphy, R.W. The origin of multiple clones in the parthenogenetic
338 lizard species *Darevskia rostombekowi*. *PloS one*, 2017, 12(9), e0185161.
- 339 13. Darevsky, I.S. & Danielyan, F.D. A study of the degree of genetic homogeneity in the
340 *Lacerta unisexualis* Darevsky, using skin graft technique. *Proceedings of the Zoological*
341 *Institute of the USSR Academy of Sciences*, Leningrad, 1979, 89: 65-70. (In Russian)
- 342 14. Danielyan, F.D. Study of mixed populations of three parthenogenetic species of the Rock
343 Lizards (*Lacerta saxicola* complex) in Armenia. *Proc. Zool. Inst.* 1987, 158, 77–83. (In
344 Russian)
- 345 15. Korkiya, I.K. Study of transplantation immunity in the Caucasian rock lizards *Lacerta*
346 *saxicola* Eversmann. *Izvestiya Akademii Nauk Gruzinská SSR, Seriya Biologicheskaya*,
347 Tbilisi, 1976, 2 (3): 243-248.
- 348 16. Uzzell, T.; Darevsky, I.S. The evidence of the hybrid origin of parthenogenetic Caucasian
349 rock lizards of the *Lacerta* genus. *Zhurnal Obshech Biol.* 1974, 35, 553–561. (In Russian)
- 350 17. Uzzell, T.; Darevsky, I.S. Biochemical evidence for the hybrid origin of the parthenogenetic
351 species of the *Lacerta saxicola* complex (*Sauria, Lacertidae*), with a discussion of some
352 ecological and evolutionary implications. *Copeia* 1975, 2, 204–222.
- 353 18. MacColloch, R.D.; Fu, J.; Darevsky, I.S.; Danielyan, F.D.; Murphy, R.W. Allozyme
354 variation in three closely related species of Caucasian rock lizards (*Lacerta*). *Amphibia-*
355 *Reptilia*, 1995, 16 (4): 331-340.
- 356 19. Fu, J.; Murphy, R.W.; Darevsky, I.S. Towards the phylogeny of Caucasian rock lizards:
357 implications from mitochondrial DNA gene sequences. *Zoological Journal of the Linnean*
358 *Society*, 1997, 120 (4): 463-477.
- 359 20. Khan, N.G.; Petrosyan, V.G.; Martirosyan, I.A.; Ryskov, A.P.; Darevsky, I.S.; Danielyan,
360 F.D.; Ryabinin, D.M.; Grechko, V.V.; Tokarskaya, O.N. Genomic polymorphism of mini-
361 and microsatellite loci of the parthenogenetic *Lacerta dahli* revealed by DNA
362 fingerprinting. *Molecular Biology*, Moscow, 1998, 32: 672-678.

- 363 21. Tokarskaya, O.N.; Kan, N.G.; Petrosyan, V.G.; Martirosyan, I.A.; Grechko, V.V.;
364 Danielyan, F.D.; Darevsky, I.S.; Ryskov, A.P. Genetic variation in parthenogenetic
365 Caucasian rock lizards of the genus *Lacerta* (*L. dahli*, *L. armeniaca*, *L. unisexualis*) analyzed
366 by DNA fingerprinting. *Mol. Genet. Genom.* 2001, 265, 1617–4615.
- 367 22. Grechko, V.V.; Ciobanu, D.G.; Darevsky, I.S.; Kosushkin, S.A.; Kramerov, D.A. Molecular
368 evolution of satellite DNA repeats and speciation of lizards of the genus *Darevskia* (*Sauria*:
369 *Lacertidae*). *Genome*, 2006, 49 (10): 1297–1307.
- 370 23. Omelchenko, A.V.; Girnyk, A.E.; Osipov, F.A.; Vergun, A.A.; Petrosyan, V.G.; Danielyan,
371 F.D.; Arakelyan M.S.; Ryskov, A.P. Genetic differentiation among natural populations of
372 the lizard complex *Darevskia raddei* as inferred from genome microsatellite marking.
373 *Russian journal of genetics*, 2016, 52(2), 231-235.
- 374 24. Moritz, C.; Donnellan, S.; Adams, M.; Baverstock, P.R. The origin and evolution of
375 parthenogenesis in *Heteronotia binoei* (*Gekkonidae*): Extensive genotypic diversity among
376 parthenogens. *Evolution*, 1989, 43, 994–1003.
- 377 25. Darevsky, I. S., Kupriyanova, L. A. 1982: Rare males in parthenogenetic lizard *Lacerta*
378 *armeniaca* Mehely. - *Vertebr. Hung.*, 21 : 69-75.
- 379 26. Darevsky, I.S.; Kupriyanova, L.A.; Danielyan, F.D. New evidence of hybrid males of
380 parthenogenetic species. In *Studies in Herpetology*; Rocek, Z., Ed.; Charles University:
381 Prague, Czech Republic, 1986; pp. 207–212.
- 382 27. Kalikinskaya, E. I., Kolomiets, O. L., Shevchenko, V. A., & Bogdanov, Y. F. Chromosome
383 aberrations in F1 from irradiated male mice studied by their synaptonemal
384 complexes. *Mutation Research Letters*, 1986, 174(1), 59-65.
- 385 28. Navarro, J.; Vidal, F.; Guitart, M.; Egozcue, J. A method for the sequential study of
386 synaptonemal complexes by light and electron microscopy. *Human genetics*, 1981, 59(4),
387 419-421.
- 388 29. Ford, C.E.; Hamerton, J.L. A colchicine hypotonic citrate squash sequence for mammalian
389 chromosomes. *Stain Technol.* 1956, 31, 247–251.
- 390 30. Zickler, D., & Kleckner, N. (1999). Meiotic chromosomes: integrating structure and
391 function. *Annual review of genetics*, 33(1), 603-754.
- 392 31. Bogdanov Yu.F., Kolomiets O.L. 2007. Synaptonemal complex as an indicator of the
393 dynamics of meiosis and chromosome variation. Moscow. 358 p. (In Russian)
- 394 32. Rovatsos, M.; Kratochvíl, L.; Altmanová, M.; Johnson Pokorná, M. Interstitial Telomeric
395 Motifs in Squamate Reptiles: When the Exceptions Outnumber the Rule. - *PLoS ONE*,
396 2015, 10(8): e0134985
- 397 33. Spangenberg, V.; Arakelyan, M.; Galoyan, E.; Matveevsky, S., Petrosyan, R., Bogdanov, Y.,
398 Danielyan F., Kolomiets, O. Reticulate evolution of the rock lizards: Meiotic chromosome
399 dynamics and spermatogenesis in diploid and triploid males of the genus *Darevskia*. *Genes*,
400 2017, 8(6), 149.
- 401 34. Rocchi, M.; Archidiacono, N.; Schempp, W.; Capozzi, O.; Stanyon, R. Centromere
402 repositioning in mammals. *Heredity*, 2012, 108(1), 59.
- 403 35. Allshire, R.C.; Karpen, G.H. Epigenetic regulation of centromeric chromatin: old dogs, new
404 tricks? *Nature Reviews Genetics*, 2008, 9(12), 923.
- 405 36. Black, B.E.; Cleveland, D. W. Epigenetic centromere propagation and the nature of CENP-a
406 nucleosomes. *Cell*, 2011, 144(4), 471-479.
- 407 37. Perpelescu, M.; Fukagawa, T. The abcs of cenps. *Chromosoma*, 2011, 120(5), 425.

- 408 38. Shang, W.H.; Hori, T.; Martins, N.M.; Toyoda, A.; Misu, S.; Monma, N.; Ikeo, K.; Hiratani,
409 I.; Maeshima, K.; Martins, N.M.C.; Earnshaw, W.C.; Kimura, H. Chromosome engineering
410 allows the efficient isolation of vertebrate neocentromeres. *Developmental cell*, 2013, 24(6),
411 635-648.
- 412 39. Zhao, H.; Zeng, Z.; Koo, D.H.; Gill, B. S.; Birchler, J. A.; Jiang, J. Recurrent establishment
413 of de novo centromeres in the pericentromeric region of maize chromosome 3. *Chromosome*
414 *Research*, 2017, 25(3-4), 299-311.
- 415 40. Stimpson, K. M.; Matheny, J. E.; Sullivan, B. A. Dicentric chromosomes: unique models to
416 study centromere function and inactivation. *Chromosome research*, 2012, 20(5), 595-605.
- 417 41. Lopez, V.; Barinova, N.; Onishi, M.; Pobiega, S.; Pringle, J. R.; Dubrana, K.; Marcand, S.
418 Cytokinesis breaks dicentric chromosomes preferentially at pericentromeric regions and
419 telomere fusions. *Genes & development*, 2015, 29(3), 322-336.
- 420 42. Earnshaw, W.C.; Migeon, B.R. Three related centromere proteins are absent from the
421 inactive centromere of a stable isodicentric chromosome. *Chromosoma*, 1985, 92(4), 290-
422 296.
- 423 43. Valente, L.P.; Silva, M. C.; Jansen, L.E. Temporal control of epigenetic centromere
424 specification. *Chromosome research*, 2012, 20(5), 481-492.
- 425 44. Voullaire, L.E.; Slater, H.R.; Petrovic, V.; Choo, K.H. A functional marker centromere with
426 no detectable alpha-satellite, satellite III, or CENP-B protein: activation of a latent
427 centromere? *American journal of human genetics*, 1993, 52(6), 1153.
- 428 45. Warburton, P.E.; Cooke, C.A.; Bourassa, S.; Vafa, O.; Sullivan, B.A.; Stetten, G.; Gimelli,
429 G.; Warburton, D.; Tyler-Smith, C.; Sullivan, K.F.; Poirier, G.G.; Earnshaw, W.C.
430 Immunolocalization of CENP-A suggests a distinct nucleosome structure at the inner
431 kinetochore plate of active centromeres. *Current Biology*, 1997, 7(11), 901-904.
- 432 46. Moens, P.B. Zebrafish: chiasmata and interference. *Genome*, 2006, 49(3), 205-208.
- 433 47. Brenner, S.; Pepper, D.; Berns, M. W.; Tan, E.; Brinkley, B. R. Kinetochore structure,
434 duplication, and distribution in mammalian cells: analysis by human autoantibodies from
435 scleroderma patients. *The Journal of Cell Biology*, 1981, 91(1), 95-102.
- 436 48. Oppedisano, L.; Haines, G.; Hrabchak, C.; Fimia, G.; Elliott, R.; Sassone-Corsi, P.;
437 Varmuza, S. The rate of aneuploidy is altered in spermatids from infertile mice. *Human*
438 *Reproduction*, 2002, 17(3), 710-717.
- 439 49. Chambon, J.P.; Touati, S.A.; Berneau, S.; Cladière, D.; Hebras, C.; Groeme, R.; McDougall,
440 A.; Wassmann, K. The PP2A inhibitor I2PP2A is essential for sister chromatid segregation
441 in oocyte meiosis II. *Current Biology*, 2013, 23(6), 485-490.

Figure 1

The spread nuclei of the leptotene-zygotene spermatocytes.

D. portschinskii (**A, C**) and *D. raddei* (**B, D**) immunostained with antibodies against the SYCP3 protein (green), anti-kinetochore ACA antibodies (red), chromatin stained with DAPI (blue). (**A, C**) -*D. portschinskii*, on each of the 19 SCs only one centromere signal is visible. (**B, D**) - *D. raddei*, additional anti-kinetochore proteins antibodies signals are indicated with arrows. Bar=5 μ m.

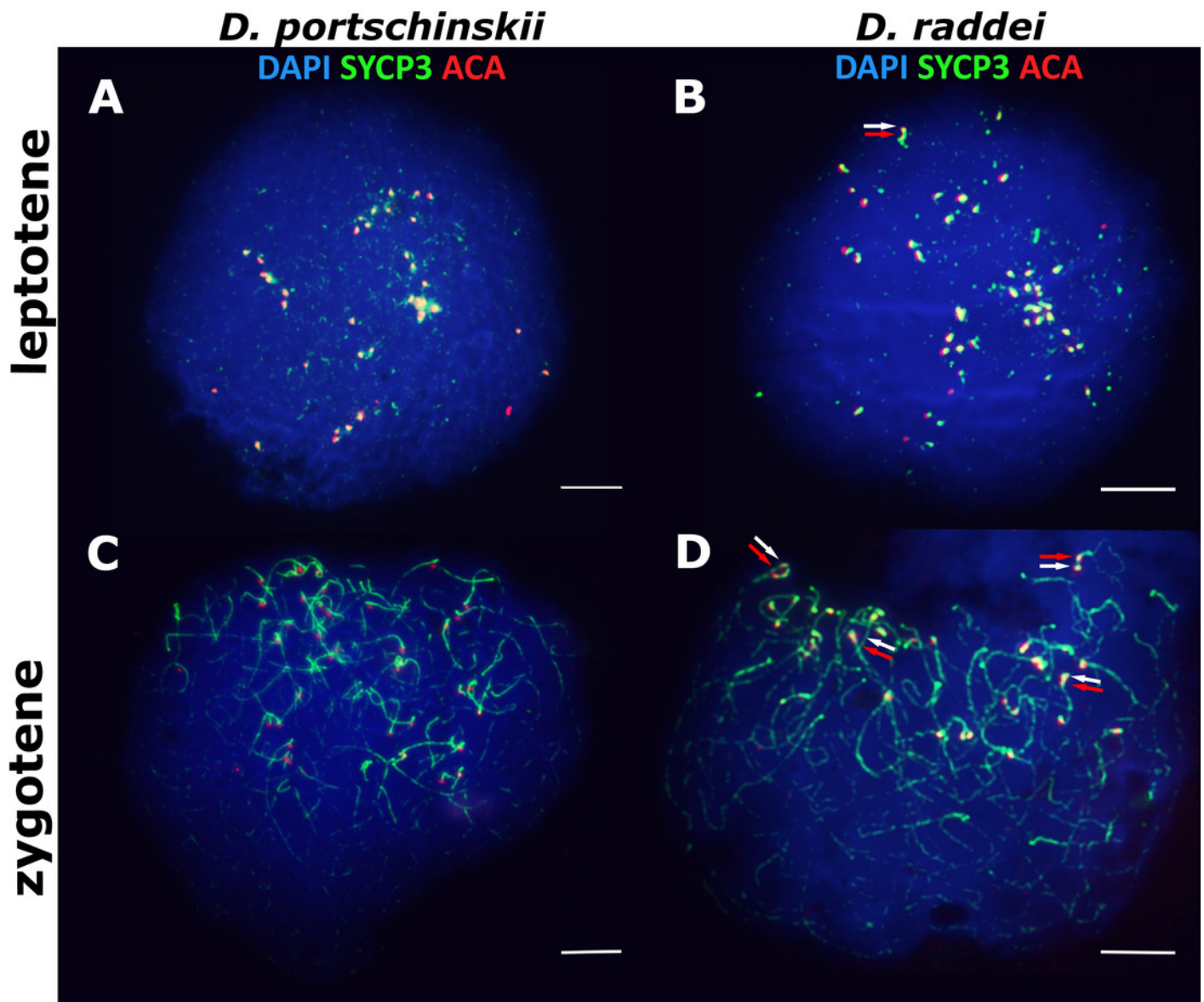


Figure 2

D. raddei synaptonemal complexes, zygotene stage.

A - SC bivalent with incomplete synapsis of pericentromeric region; D - SC bivalents during the elongation of synapsis. Immunostaining with antibodies against the SYCP3 protein (green), ACA - anti-kinetochore proteins antibodies (red). Additional ACA-signals indicated with arrows. Enlarged fragments (B, C, E) demonstrate additional ACA foci on each axial element prior to synapsis. Bar = 5 μ m.

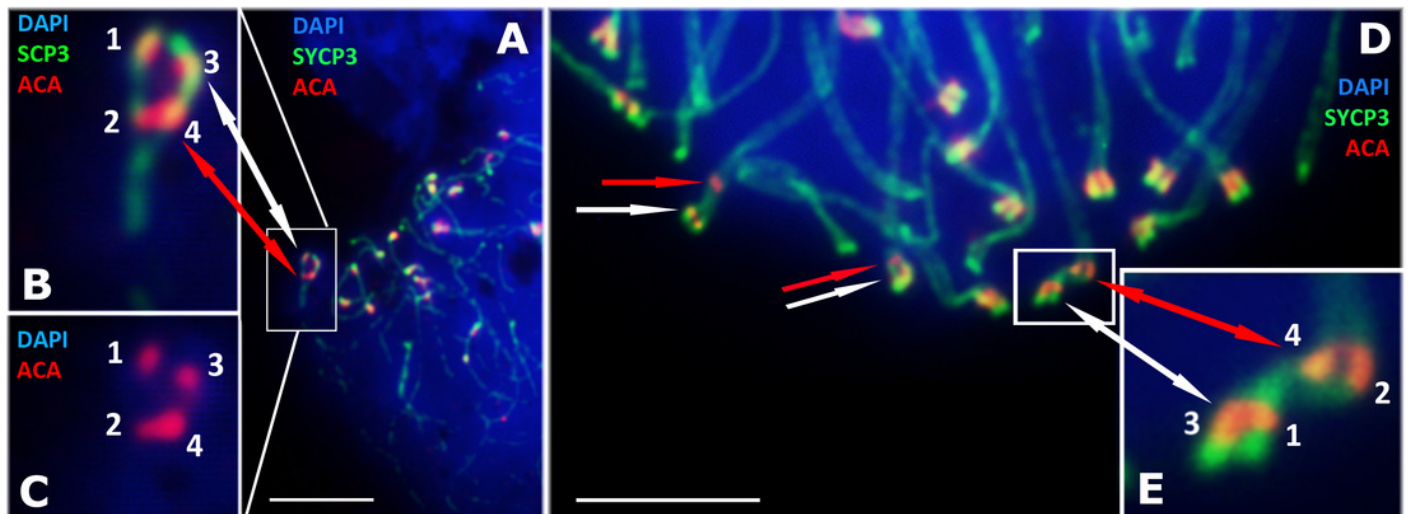


Figure 3

The spread nuclei of the pachytene-diplotene spermatocytes.

The spread nuclei of the pachytene-diplotene spermatocytes. *D. portschinskii* (**A,C**) and *D. raddei* (**B,D**) immunostained with antibodies against the SYCP3 protein (green), anti-kinetochore ACA antibodies (red), chromatin stained with DAPI (blue). (**A, C**) -*D. portschinskii*, on each of the 19 SCs only one centromere signal is visible. (**B, D**) - *D. raddei*, additional anti-kinetochore proteins antibodies signals are indicated with arrows. Bar=5 μ m.

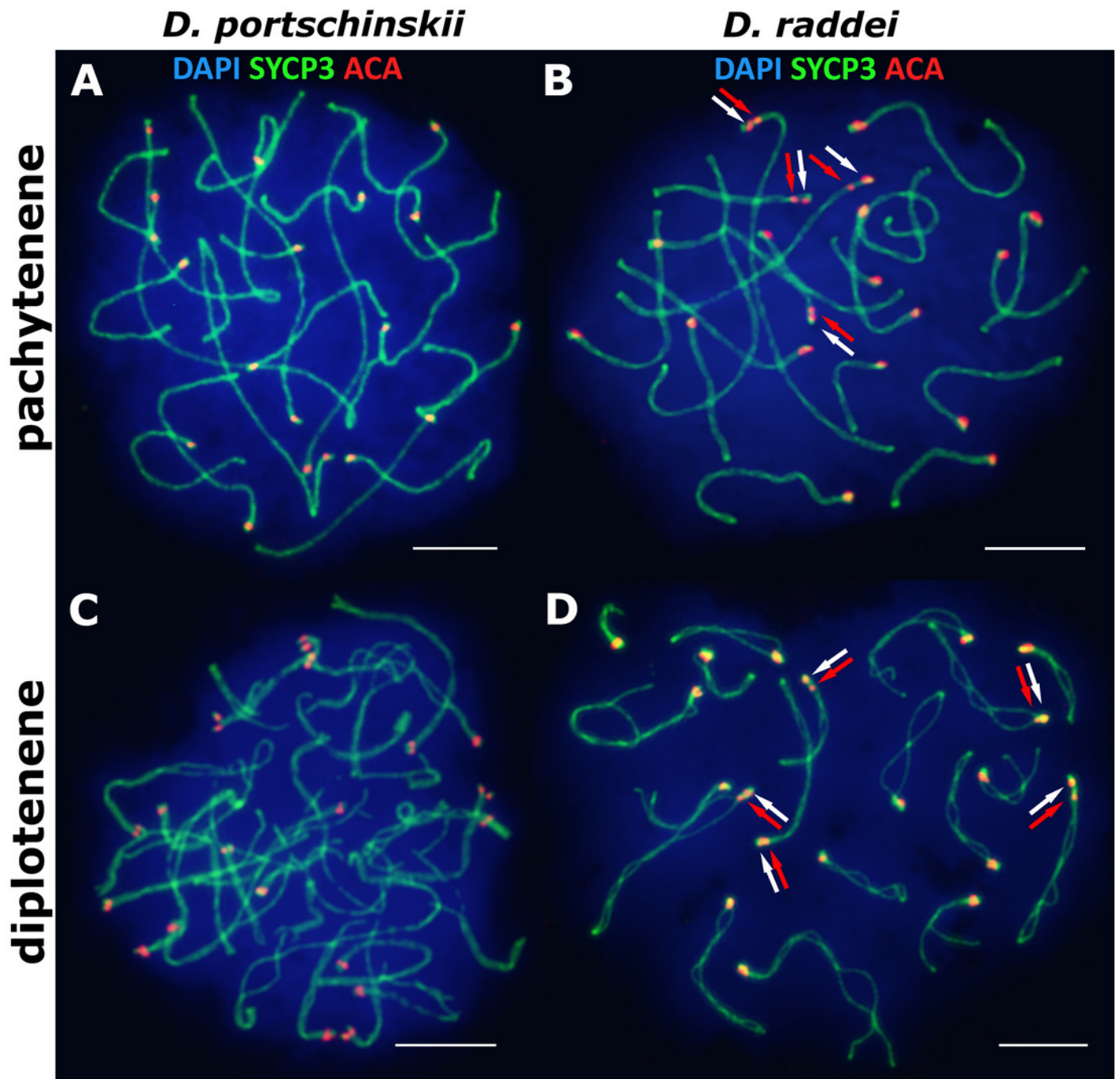


Figure 4

A comparison idiogram of average SC lengths of two species

(A) - A comparison idiogram of average SC lengths of two species: *D. portschinskii* (blue, 78 pachytene nuclei) and *D. raddei* (green, 54 pachytene nuclei). **(B)** and **(C)** - immuno-FISH, fragments of SC preparations *D. portschinskii* and *D. raddei*. **(B)** - single ACA foci in *D. portschinskii* SC bivalents; **(C)** - Additional ACA focus in *D. raddei* SC is (red arrow). Telomere FISH signals (white) are located at the ends of SC bivalents in both species and were not detected in the area of the additional ACA focus in *D. raddei*. **(D)** and **(E)** - distribution of additional ACA-foci on the 19 SC-bivalents of *D. raddei* in 54 spermatocyte nuclei studied. Bar = 2 μ m.

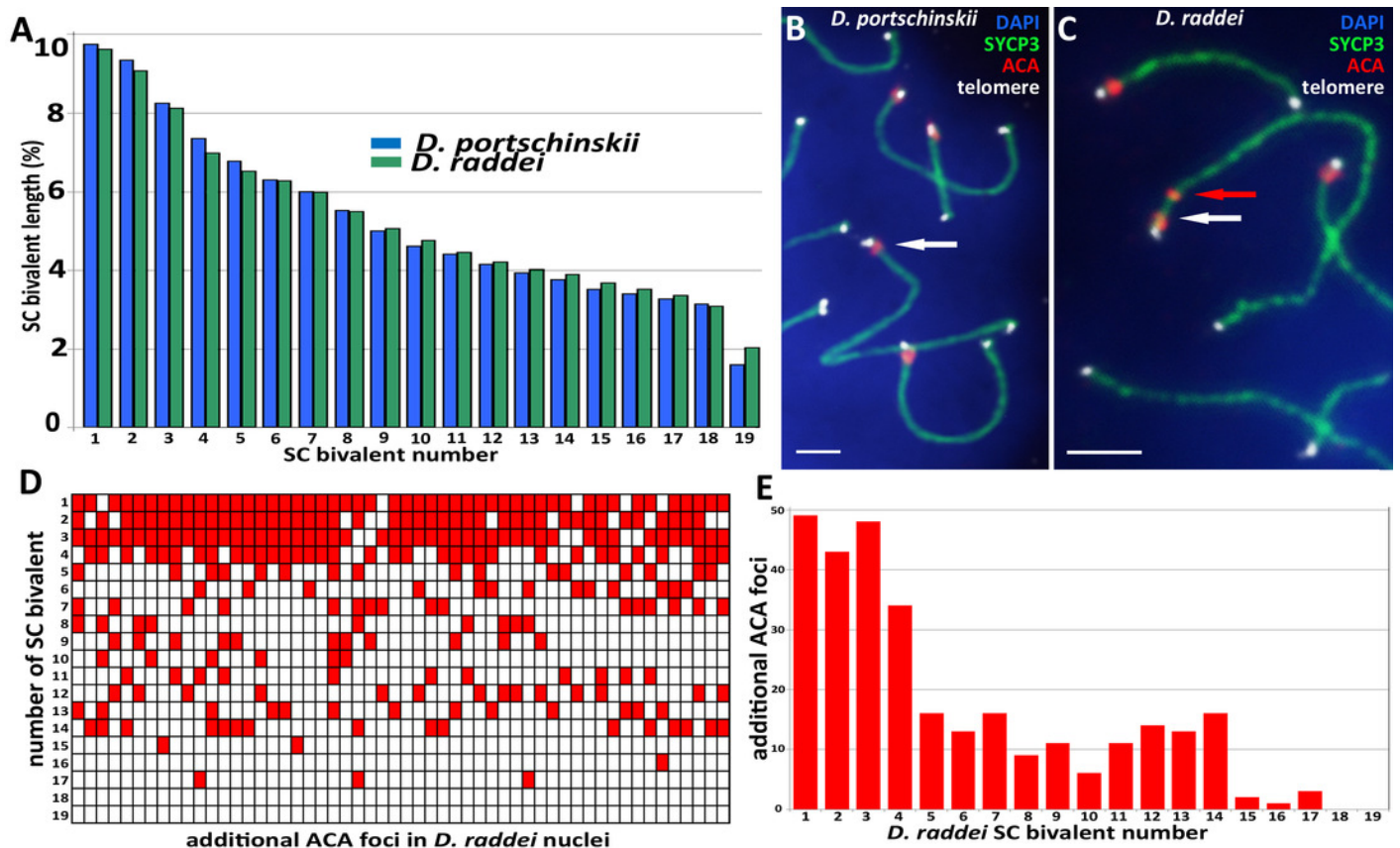


Figure 5

The spread nuclei of the pachytene spermatocyte *D. portschinskii* and *D. raddei*

The spread nuclei of the pachytene spermatocyte *D. portschinskii* (**A**) and *D. raddei* (**B**) immunostained with antibodies against the SYCP3 protein (green) - lateral elements of meiotic chromosomes, anti-kinetochore ACA antibodies (red), antibodies against mismatch repair protein MLH1 (yellow) - sites of crossing over. (**C**) - number of crossing over sites (MLH1 foci) per spermatocyte nucleus (mean \pm SD) in *D. portschinskii* and *D. raddei*. Bar = 5 μ m.

